Small-signal Stability Analysis of Power Systems under Uncertain Renewable Generation

Yuhan Zhou, Guanzhong Wang, Almir Ekic, Wei Huang, Chen Wu, Dan Zhang, Di Wu, Huanhai Xin

***Abstract* — The increasing penetration of inverter-based resources (IBRs) is changing grid dynamics and challenging safe and reliable grid operation. Particularly, the increasing integration of IBRs may cause the small-signal stability issues resulting from the dynamic interaction between the IBR inverter controls and the power network in a power system with high penetration of IBRs. It is challenging for assessing the small-signal stability in such a power system due to the complex interaction between IBRs interconnected through the power network. The assessment complexity is further increased when considering variable IBR generation. To address the challenges, this paper proposes a method for small-signal stability analysis of a multi-IBR power system under uncertain renewable generation. First, we derive that the small-signal stability of a multi-IBR power system can be estimated based on the smallest eigenvalue of a weighted Laplacian matrix of the power network. Then, a robust optimization problem is formulated to analyze the small-signal stability of a multi-IBR power system under variable renewable generation. The efficacy of the proposed method is demonstrated on a power system with three IBRs by eigenvalue analysis and electromagnetic transient simulations.**

***Index Terms*— Inverter-based resources, small-signal stability, uncertain renewable generation.**

2022 IEEE Power & Energy Society General Meeting (PESGM) | 978-1-6654-0823-3/22/$31.00 ©2022 IEEE | DOI: 10.1109/PESGM48719.2022.9916873

I. Introduction

To address the impact of climate change, renewable energy resources such as wind and solar are increasingly integrated into the nation's electric power grid to reduce reliance on fossil fuels. These renewable resources are interfaced with the power grid through power electronic inverters that use control algorithms to define their performance characteristics [1]. As a group, these types of resources are commonly referred to as inverter-based resources (IBRs). While IBRs offer fast and advanced control for energy efficiency, they are also are changing grid dynamics and challenging safe and stable grid operation. Particularly, the dynamic interaction between IBRs and the power network have cause new types of multi-frequency oscillation stability issues under weak grid connections, such as sub-/super synchronous and high-frequency oscillations [2]-[5]. The emerging oscillation stability issues are becoming a major threat to grid reliability and a great bottleneck to the accommodation of IBRs.

Since the oscillation stability issues belong to the small-signal stability category, they have mainly been investigated by time-domain [6]-[7] and frequency-domain [8]-[9] methods. The most widely used time-domain methods are the eigenvalue analysis method and the electromagnetic transient simulation. In the eigenvalue analysis method, the studied system is usually represented with state-space models and then the eigenvalue analysis method is used to analyze the small-signal stability. This method requires detailed models and parameters of inverters to build the state-space model. It is challenging for using the method in a large-scale power system with large IBR integration since the dimensions of the system state matrix may be too high to be numerically handled for eigenvalue analysis. While the electromagnetic transient simulations can be used for verification purposes, they hardly reveal the mechanism of small-signal instability. Recently, the impedance-based analysis method in the frequency domain has been used for the small-signal stability analysis as the impedance model can be obtained through measurements, even though the detailed parameters of the inverter are unknown. Although the small-signal stability has been analyzed with the various approaches in time and frequency domains, it is still challenging to analyze the stability issue while considering the impact of variable renewable generation [10]-[11]. Moreover, the analysis complexity is further increased when considering the interaction between IBRs interconnected through the power network in a multi-IBR power system.

To address the challenges, the paper proposes a method for analyzing the impact of uncertain renewable generation on the small-signal stability in a multi-IBR power system. To this end, the modeling of a multi-IBR power system is first constructed based on the state-space model. With this modeling, the small-signal stability of the system is analyzed, and then a robust optimization is formulated to assess the small-signal stability under uncertain renewable generation. The efficacy of the proposed method is demonstrated on a power system with multiple IBRs. The rest of this paper is organized as follows. In Section II, the modeling of the power system with multiple IBRs will be presented. In Section III, the model will be used to analyze the small-signal stability of the multi-IBR system. In Section IV, our method will be proposed to assess the small-signal stability of the multi-IBR system under uncertain IBR generation. In Section V, the efficacy of the proposed method will be demonstrated. In Section VI, the conclusions are drawn.

II. Modeling for Power Systems with Multiple IBRs

Let us consider a power system with n IBRs. The system modeling includes the IBR models and the network models. The state-space model of the i-th IBR can be represented as

$$\begin{cases} \dfrac{d}{dt}\Delta \boldsymbol{X}_{m,i} = \boldsymbol{A}_{m,i}\Delta \boldsymbol{X}_{m,i} + \boldsymbol{B}_{m,i}\Delta \boldsymbol{U}_{m,i} \\ \Delta \boldsymbol{I}_{m,i} = P_{Bi} \cdot \boldsymbol{C}_{m,i}\Delta \boldsymbol{X}_{m,i} \end{cases} \tag{1}$$

where Δ denotes small increment of a variable vector; $\boldsymbol{X}_{m,i} \in \mathbf{R}^{m\times 1}$ is the vector of all the state variables of i-th IBR; $\boldsymbol{I}_{m,i}=[I_{x,i}\ I_{y,i}]^T$ and $\boldsymbol{U}_{m,i}=[U_{x,i}\ U_{y,i}]^T$ are the output current and terminal

This work is supported in part by National Science Foundation Award 2033355 and ND EPSCoR STEM Research and Education Grant.

978-1-6654-0823-3/22/$31.00 ©2022 IEEE

voltage at the point i of interconnection, respectively, expressed in the common x-y coordinate; $\boldsymbol{A}_{m,i}\in\mathbf{R}^{\mathrm{m}\times\mathrm{m}}$ and $\boldsymbol{B}_{m,i}\in\mathbf{R}^{\mathrm{m}\times 2}$ are the state matrix and control matrix of the i-th IBR, respectively; and $\boldsymbol{C}_{m,i}\in\mathbf{R}^{2\times\mathrm{m}}$ is the output matrix of the i-th IBR, which is normalized by the injected power $P_{B,i}$ of the i-th IBR.

Based on (1), the state-space model of the i-th IBR can be rewritten in the following matrix format:

$$\begin{bmatrix}\mathbf{0}^{m\times 1}\\ \Delta\boldsymbol{I}_{m,i}\end{bmatrix}=\begin{bmatrix}s\boldsymbol{I}_m-\boldsymbol{A}_{m,i} & -\boldsymbol{B}_{m,i}\\ P_{Bi}\boldsymbol{C}_{m,i} & \mathbf{0}^{2\times 2}\end{bmatrix}\begin{bmatrix}\Delta\boldsymbol{X}_{m,i}\\ \Delta\boldsymbol{U}_{m,i}\end{bmatrix} \tag{2}$$

where $\mathbf{0}^{\mathrm{m}\times 1}$ and $\mathbf{0}^{2\times 2}$ are two null matrices; s represents Laplace operator; and $\boldsymbol{I}_m$ denotes the m-dimensional identity matrix.

Thus, the state-space model of the power system with n IBRs can be represented as

$$\begin{bmatrix}\mathbf{0}^{nm\times 1}\\ \Delta\boldsymbol{I}_m\end{bmatrix}=\begin{bmatrix}diag\left(s\boldsymbol{I}_m-\boldsymbol{A}_{m,i}\right) & diag\left(-\boldsymbol{B}_{m,i}\right)\\ diag\left(S_{Bi}\cdot\boldsymbol{C}_{m,i}\right) & \mathbf{0}^{2n\times 2n}\end{bmatrix}\begin{bmatrix}\Delta\boldsymbol{X}_m\\ \Delta\boldsymbol{U}_m\end{bmatrix},\ i=1,\ldots,n \tag{3}$$

$$\Delta\boldsymbol{X}_m=\begin{bmatrix}\Delta\boldsymbol{X}_{m,1}^T & \cdots & \Delta\boldsymbol{X}_{m,n}^T\end{bmatrix}^T$$

$$\Delta\boldsymbol{I}_m=\begin{bmatrix}\Delta\boldsymbol{I}_{m,i}^T & \cdots & \Delta\boldsymbol{I}_{m,n}^T\end{bmatrix}^T$$

$$\Delta\boldsymbol{U}_m=\begin{bmatrix}\Delta\boldsymbol{U}_{m,1}^T & \cdots & \Delta\boldsymbol{U}_{m,n}^T\end{bmatrix}^T$$

where $\mathbf{0}^{\mathrm{nm}\times 1}$ and $\mathbf{0}^{2\mathrm{n}\times 2\mathrm{n}}$ are two null matrices; symbol diag(·) represents the diagonal matrix.

By eliminating $\Delta\boldsymbol{X}_m$ in (3) through the Kron reduction [12], the relationship between $\Delta\boldsymbol{I}_m$ and $\Delta\boldsymbol{U}_m$ at the IBR terminals in (3) can be represented

$$\Delta\boldsymbol{I}_m=diag\left[P_{Bi}\cdot\boldsymbol{Y}_{IBR\_i}(s)\right]\Delta\boldsymbol{U}_m\ ,\ i=1,\ldots,n \tag{4}$$

where

$$\boldsymbol{Y}_{IBR\_i}(s)=\boldsymbol{C}_{m,i}\left(s\boldsymbol{I}_m-\boldsymbol{A}_{m,i}\right)^{-1}\boldsymbol{B}_{m,i} \tag{5}$$

In the power system with n IBRs, the power network interconnecting n IBRs can be modeled:

$$-\Delta\boldsymbol{I}_m=\left[\boldsymbol{B}\otimes\gamma(s)\right]\Delta\boldsymbol{U}_m \tag{6}$$

where

$$\gamma(s)=\begin{bmatrix}\beta(s) & \alpha(s)\\ -\alpha(s) & \beta(s)\end{bmatrix},\qquad \alpha(s)=\frac{\omega_0^2}{s^2+\omega_0^2},\ \beta(s)=\frac{s\omega_0}{s^2+\omega_0^2} \tag{7}$$

where $\boldsymbol{B}$ is the reduced node susceptance matrix after eliminating passive nodes and infinite nodes; ω_0 is the rated angular velocity of the ac system; and $\otimes$ denotes the Kronecker product.

By integrating the IBR modeling (4) and the power network modeling (6), the power system with n IBRs can be modeled by an equivalent multi-input multi-output feedback control system as shown in Fig. 1 below. The closed-loop characteristic equation of the system can be represented by

$$\det\left(diag\left[P_{Bi}\cdot\boldsymbol{Y}_{IBR\_i}(s)\right]+\boldsymbol{B}\otimes\gamma(s)\right)=0 \tag{8}$$

where det(·) denotes the determinant function. The system is stable if and only if all the eigenvalues of (8) are in the left-half of the complex plane.

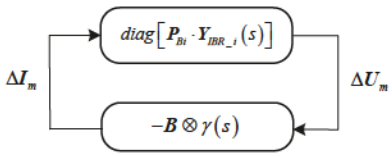

Fig. 1 Closed-loop diagram of the power system with n IBRs.

III. Small-Signal Stability Analysis of Power Systems with Multiple IBRs

The closed-loop characteristic equation (8) allows us to analyze the small-signal stability of the power system with n IBRs. To simplify this analysis, let us consider each IBR in the system has the same dynamic control strategy and parameters. That is, $\boldsymbol{A}_{m,i}=\boldsymbol{A}_m$, $\boldsymbol{B}_{m,i}=\boldsymbol{B}_m$, $\boldsymbol{C}_{m,i}=\boldsymbol{C}_{m,i}$, i =1,…, n, in (8). Under this condition, the closed-loop characteristic equation (8) can be rewritten:

$$\det\left[\boldsymbol{Y}_{\mathrm{hom}\_sys}\right]=\det\left[\left(\boldsymbol{I}_n\otimes\boldsymbol{Y}_{IBR}(s)\gamma(s)^{-1}\right)+\boldsymbol{Y}_{eq}\otimes\boldsymbol{I}_2\right]=0 \tag{9}$$

where

$$\boldsymbol{Y}_{IBR}(s)=\boldsymbol{C}_m\left(s\boldsymbol{I}_m-\boldsymbol{A}_m\right)^{-1}\boldsymbol{B}_m\,, \tag{10}$$

where $\boldsymbol{Y}_{eq}=\boldsymbol{P}_{\mathrm{B}}^{-1}\boldsymbol{B}$; $\boldsymbol{P}_{\mathrm{B}}=\mathrm{diag}(P_{\mathrm{Bi}})$, i=1,…,n; $\boldsymbol{I}_n$ is a n-dimension identity matrix.

Equation (9) characterizes the small-signal stability of the power system interconnecting n IBRs through the power network in the multi-IBR power system. The interaction between n IBRs will increases the complexity of the small-signal stability analysis in the system. To reduce the analysis complexity, we will decouple the n-IBR system into a set of single-IBR subsystems based on the following Lemma 1:

Lemma 1. matrix $\boldsymbol{Y}_{eq}$ is diagonalizable, and its all eigenvalues are positive.

Proof: In a power system with n IBRs, P_{Bi} in matrix $\boldsymbol{P}_{\mathrm{B}}$ meets $P_{Bi}>0$, i=1,…,n. Thus, $P_B^{-1/2}$ are positive definite. As matrix $\boldsymbol{B}$ is a Hermitian diagonally dominant matrix with positive diagonal entries, $\boldsymbol{B}$ is positive definite in (6), and then the $\boldsymbol{P}_B^{-1/2}\boldsymbol{B}\boldsymbol{P}_B^{-1/2}$ is positive definite. Since $\boldsymbol{P}_B^{1/2}\boldsymbol{Y}_{eq}\boldsymbol{P}_B^{-1/2}=\boldsymbol{P}_B^{-1/2}\boldsymbol{B}\boldsymbol{P}_B^{-1/2}$, $\boldsymbol{Y}_{eq}$ is similar to $\boldsymbol{P}_B^{-1/2}\boldsymbol{B}\boldsymbol{P}_B^{-1/2}$ and is positive definite matrix. Thus, $\boldsymbol{Y}_{eq}$ is diagonalizable and its eigenvalues are all positive. This concludes the proof ■.

According to Lemma 1, there is a matrix $\boldsymbol{W}$ that can decompose matrix $\boldsymbol{Y}_{eq}$ into a diagonal matrix in which the diagonal elements consist of the eigenvalues (σ_i, i=1,…,n) in the order of $0\leqslant\sigma_1\leqslant\sigma_2\cdots\leqslant\sigma_n$. That is,

$$\boldsymbol{W}^{-1}\boldsymbol{Y}_{eq}\boldsymbol{W}=\boldsymbol{\Lambda}=diag(\sigma_i)\ \ i=1,\ldots,n \tag{11}$$

Combining (11) with (9) yields,

$$\prod_{i=1}^{n}\det\left(\boldsymbol{Y}_{IBR}(s)\gamma(s)^{-1}+\sigma_i\otimes\boldsymbol{I}_2\right)=0 \tag{12}$$

Equation (12) shows that the power system with n IBRs can be decoupled into n dynamically independent subsystems for the small-signal stability analysis. The multi-IBR system is stable if and only if all the equivalent subsystems are stable. In other words, if one of the equivalent subsystems is unstable, the entire system will be unstable. In the multi-IBR system, each IBR has the same dynamic control strategy and parameters. For the given control strategy and parameters, the

978-1-6654-0823-3/22/$31.00 ©2022 IEEE

stability of each subsystem depends on the eigenvalues σ_i (i=1,…,n). The smaller eigenvalue σ_i means its corresponding subsystem is more likely to be unstable. The smallest eigenvalue σ_1 is corresponding the subsystem, which is the most critical. Thus, the small-signal stability of the entire system depends on the critical subsystem, and the stability of the entire multi-IBR system can be characterized by the smallest eigenvalue σ_1.

IV. Proposed Method for Small-signal Stability Assessment under Uncertain Renewable Generation

According to the small-signal stability analysis in the Section III, it is known that the small-signal stability of the power system with n IBRs can be assessed based on the smallest eigenvalue σ_1 of weighted matrix $\boldsymbol{Y}_{eq}$ in (9) for the power network. However, matrix $\boldsymbol{Y}_{eq}$ is the function of IBR generation $\boldsymbol{P}_B$. When IBR generation is uncertain, the small-signal stability assessment based on the smallest eigenvalue σ_1 is required for all feasible uncertain scenarios, which is computationally daunting.

To address this issue, a robust optimization model can be formulated for assessing the small-signal stability in the worst-scenario under uncertain IBR generation based on the smallest eigenvalue σ_1 of matrix $\boldsymbol{Y}_{eq}$. If under the worst scenario the power grid stable, all other uncertain scenarios are also stable. To this end, let $\Delta \in \boldsymbol{R}^n$ be an uncertain set, and the IBR generation is constrained within Δ (i.e., $\boldsymbol{P}_B \in \Delta$). For the power system with n IBRs, when its power network parameters are given, matrix $\boldsymbol{Y}_{eq}$ only changes with IBR generation $\boldsymbol{P}_B$ (i.e., $\boldsymbol{Y}_{eq}(\boldsymbol{P}_B)$). Thus, the smallest eigenvalue of matrix $\boldsymbol{Y}_{eq}(\boldsymbol{P}_B)$ under uncertainty is defined as $\sigma_{\min}=\min\{\Lambda(\boldsymbol{Y}_{eq}(\boldsymbol{P}_B)): \boldsymbol{P}\in\Delta\}$, where $\Lambda(\cdot)$ is the function to yield the eigenvalues of a given matrix. Let γ be a given threshold to guarantee dynamic control stability of a power grid. When $\sigma_{\min}>\gamma$, every uncertain scenario must be stable. Equivalently, the stability identification based on the $\sigma_{\min}$ is to verify if all eigenvalues of $\boldsymbol{Y}_{eq}(\boldsymbol{P}_B)$ under uncertainty Δ are larger than threshold γ. Thus, the small-signal stability under uncertainty Δ can be analyzed by solving the following optimization problem to verify if all eigenvalues of $\boldsymbol{Y}_{eq}(\boldsymbol{P}_B)$ are in the subset H for $\boldsymbol{P}_B\in\Delta$, where $H=(\gamma,\infty)$ is an open subset of the complex plane, and its complement $H^c=(0,\gamma)$ is a semi-algebraic set.

$$\max_{x\in\boldsymbol{R}^n,\boldsymbol{P}_B\in\Delta,\gamma\in\boldsymbol{R}} \|x\|_2^2 \tag{13}$$

$$s.t.\ (\boldsymbol{Y}_{eq}(\boldsymbol{P}_B)-\sigma I_n)x=0 \tag{14}$$

$$\|x\|_2^2\le 1,\ \sigma\in H^c \tag{15}$$

Equations (13)-(15) show that if all eigenvalues of matrix $\boldsymbol{Y}_{eq}(\boldsymbol{P}_B)$ are located in subset H, there exists no $\sigma\in H^c$ and $\boldsymbol{P}_B\in\Delta$, which make the matrix $(\boldsymbol{Y}_{eq}(\boldsymbol{P}_B)-\sigma\boldsymbol{I}_n)$ singular. Thus, only the trivial solution x=0 satisfies the constraint (14). That is, the system is stable under uncertain IBR generation $\boldsymbol{P}_B\in\Delta$ if the solution of the problem in (13)-(15) is equal to zero. To solve this problem in (3)-(5), this problem can be converted into an optimization problem with linear matrix inequality (LMI) constraints, and then solve the converted problem by building up LMI relaxations to relax the optimization problem into a sequence of semidefinite optimization problems [13].

V. Case Studies

In this section, the efficacy of the proposed method is demonstrated on a power system with three IBRs by eigenvalue analysis and electromagnetic transient simulations. The system topology is shown in Fig. 2 while the network parameters of the system are presented in Table I. All inverters use the same control strategy shown in Fig. 3, and the control parameters of each inverter are shown in Table II. In the system, let us consider the injected power P_i (i=1,2,3) of each IBR varies in the interval (0, 2) p.u.. The varying generation of these three IBRs can be illustrated by a cube in a three-dimensional space, which is shown in Fig.4. In this figure, the cube is divided into 8 sub cubes numbered as ①~⑧ for validating the proposed method.

In the system, the proposed optimization problem in (13)-(15) is solved under variable IBR generation. For the given inverter control strategy and parameters in the system, we can evaluate the threshold value γ=3.1 for the proposed optimization problem (13)-(15) by either analytical calculation or numerical simulation method. Thus, semi-algebraic set H^c in (15) is (0, 3.1). Table III presents the solutions to optimization problem in (13)-(15) under different scenarios of variable IBR generation Δ_i (i=1,…, 8) as illustrated in Fig. 4. It can be seen from Table III that the system is stable under scenarios Δ_1~Δ_2 and Δ_4~Δ_8, but there is an instability risk in the system under scenario Δ_3. As shown in Table III, the solutions to the optimization problem is 0 under scenarios Δ_1~Δ_2 and Δ_4~Δ_8, which means the system is stable under these scenarios of variable IBR generation; on the other hand, the solutions to the optimization problem is 1 under scenario Δ_3, which indicates these exits an instability risk under this scenario.

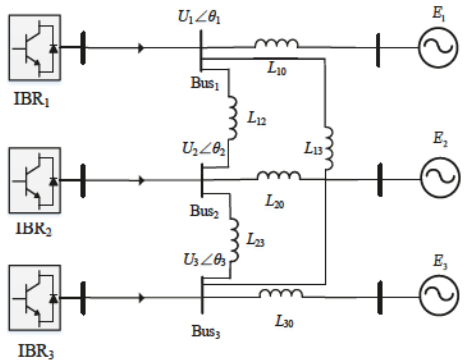

Fig. 2 Diagram of the power system with three IBRs

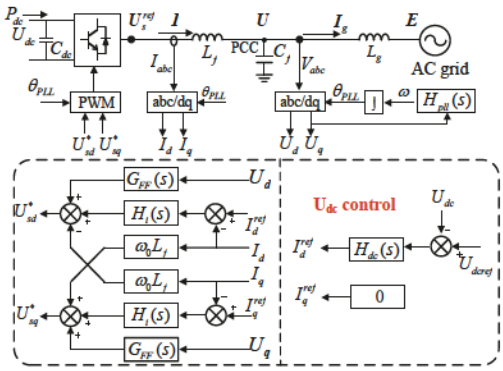

Fig. 3 The control block diagram of IBR inverter used in the system in Fig. 2

978-1-6654-0823-3/22/$31.00 ©2022 IEEE

Table I Network parameters of the system shown in Fig. 2 in per unit

L_{10}	0.25	L_{20}	0.20	L_{30}	0.15
L_{12}	0.20	L_{13}	0.15	L_{23}	0.10

Table II Parameters of IBRs in the system shown in Fig. 2

PI parameters of current control loop: 1, 10
PI parameters of the constant DC voltage control loop: 0.5, 5
Parameters of the voltage feedforward filter: 0.01
PI parameters of the PLL: 20, 7500
Parameters of active power output and q-axis current reference: 1, 0
Rated capacity of converters in per unit: 1

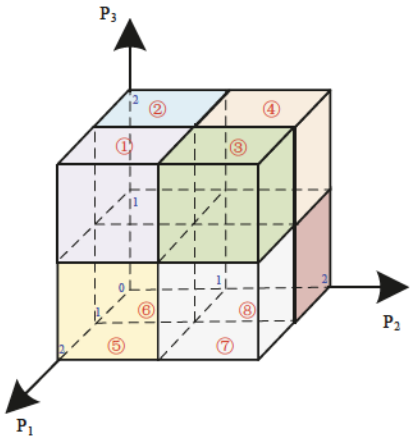

Fig. 4 The cube related to the uncertain IBR generation in the system shown in Fig. 2

Table III The solutions to optimization problem (14)-(16) in the system shown in Fig. 2 under different scenarios of variable IBR generation

IBR generation scenarios	Solutions to optimization problem (14)-(16)
Δ_1=((1,2),(0,1),(1,2))	0
Δ_2=((0,1),(0,1),(1,2))	0
Δ_3=((1,2),(1,2),(1,2))	1
Δ_4=((0,1),(1,2),(1,2))	0
Δ_5=((1,2),(0,1),(0,1))	0
Δ_6=((0,1),(0,1),(0,1))	0
Δ_7=((1,2),(1,2),(0,1))	0
Δ_8=((0,1),(1,2),(0,1))	0

To validate the solutions to the proposed optimization problem in Table III, eigenvalue analysis is first conducted by MATLAB/Simulink in the system under these scenarios of variable IBR generations. In the eigenvalue analysis, many different IBR generation conditions in the system is randomly selected under each of these 8 scenarios listed in Table III. Under each selected IBR generation condition, the eigenvalue analysis is carried out. Table IV demonstrates the typical results of eigenvalue analysis in the system under each scenario. As observed from Table IV, the dominant eigenvalues of the system under scenarios Δ_1~Δ_2 and Δ_4~Δ_8 are located in the left-half complex plane, which indicates the system is stable. On the other hand, the dominant eigenvalues of the system under scenario Δ_3 are located in the right-half complex plane, which indicates there is an instability risk in the system. The analysis results are consistent with the solutions to the proposed optimization problem in Table III. Thus, the proposed method is validated.

Further, electromagnetic transient simulations are performed by MATLAB/Simulink to validate the solutions in Table III. In the simulations, many different IBR generation conditions in the system is also randomly chosen under each of these 8 scenarios listed in Table III. Under each chosen IBR generation condition, the electromagnetic transient simulation is conducted. Fig. 5 demonstrates the typical simulation results in the system under each scenario. It can be observed from Fig. 5, the voltage trajectories at three IBR buses in the system under scenarios Δ_1~Δ_2 and Δ_4~Δ_8 are convergent, which indicates the system is stable. By contrast, the voltage trajectories at three IBR buses in the system under scenario Δ_3 are divergent, which indicates there exists an instability risk in the system. Again, the analysis results agree with the solutions to the proposed optimization problem in Table III, which thus validates the proposed method.

Table IV The typical results of eigenvalue analysis in the system shown in Fig. 2 under different scenarios of variable IBR generation

IBR generation scenarios	Dominant eigenvalues
Δ_1	-1.57±89.22i
Δ_2	-4.59±88.72i
Δ_3	1.18±89.26i
Δ_4	-1.92±89.19i
Δ_5	-3.78±88.91i
Δ_6	-6.76±88.00i
Δ_7	-1.33±89.24i
Δ_8	-4.26±88.80i

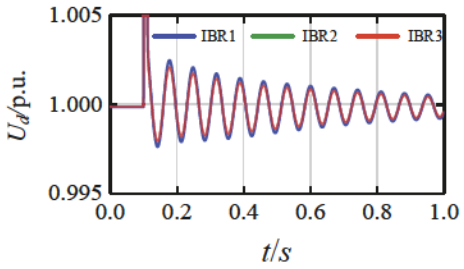

(a) Under IBR generation scenario Δ_1

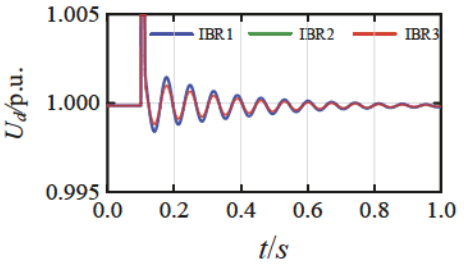

(b) Under IBR generation scenario Δ_2

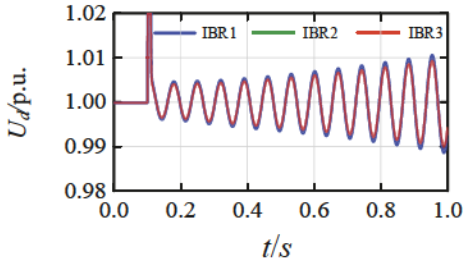

(c) Under IBR generation scenario Δ_3

978-1-6654-0823-3/22/$31.00 ©2022 IEEE

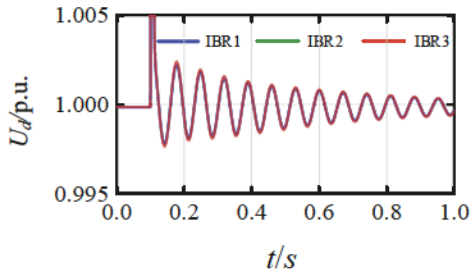

(d) Under IBR generation scenario Δ_4

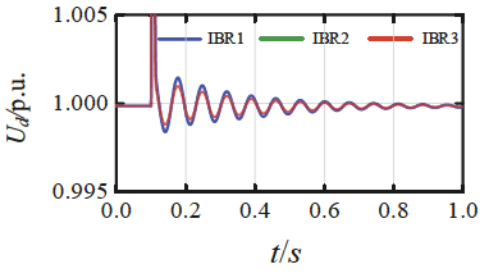

(e) Under IBR generation scenario Δ_5

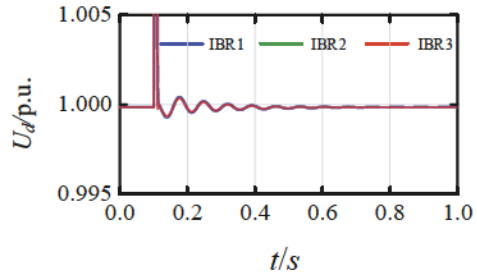

(f) Under IBR generation scenario Δ_6

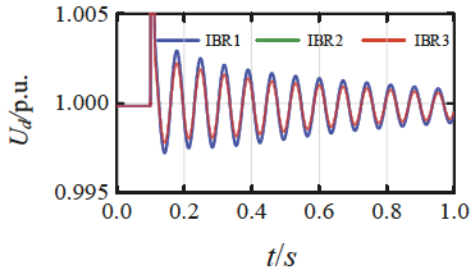

(g) Under IBR generation scenario Δ_7

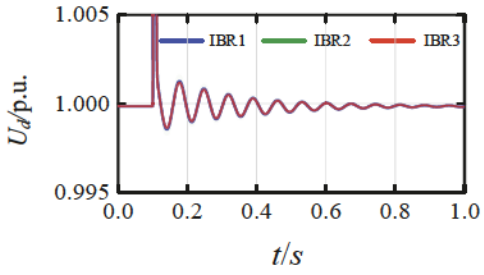

(e) Under IBR generation scenario Δ_8

Fig. 5 The typical results of voltage trajectories at IBR buses in the system shown in Fig. 2 under different scenarios of variable IBR generation

VI. Conclusion

In this paper, a method was proposed for the small-signal stability analysis of a multi-IBR power system under variable renewable generation. Due to the complex interaction between IBRs interconnected through the power network and variable renewable generation, it is challenging for the small-signal stability analysis in a multi-IBR power system. To address the challenges, it was theoretically proved that the small-signal stability can be characterized by the smallest eigenvalue of a weighted Laplacian matrix of the power network in a multi-IBR power system. On the basis, a robust optimization was formulated to assess the smallest eigenvalue under variable renewable generation for the small-signal stability analysis of a multi-IBR power system while considering under uncertain renewable generation. The efficacy of the proposed method was demonstrated on a power system with three IBRs through both electromagnetic transient simulation and modal analysis. The proposed method is helpful for grid planners and operators to understand the impact of uncertain renewable generation on the small-signal stability resulting from the interaction between IBRs and the power network in the power system with large-scale IBR integration.

VII. References

[1] "Reliability guideline: Integrating inverter-based resources into weak power systems," North Amer. Elect. Rel. Corporation, Jun. 2017. [Online].Available: http://www.nerc.com/pa/RAPA/rg/ReliabilityGuidelines

[2] L. Fan and Z. Miao, "An explanation of oscillations due to wind power plants weak grid interconnection," *IEEE Trans. Sustain. Energy*, vol. 9, no.1, pp. 488–490, Jan. 2018.

[3] H. Liu, X. Xie, J. He, "Subsynchronous interaction between direct-drive PMSG based wind farms and weak AC networks," *IEEE Trans. Power Syst.*, vol. 32, no. 6, pp. 4708-4720, Nov. 2017.

[4] L. P. Kunjumuhammed, B. C. Pal, C. Oates, et al., "Electrical oscillations in wind farm systems: analysis and insight based on detailed modeling," *IEEE Trans. Sustain. Energy*, vol. 7, no. 1, pp. 51–62, Jan. 2016.

[5] J. Zhou, H. Ding, S. Fan, Y. Zhang, and A. Gole, "Impact of short-circuit ratio and phase-locked-loop parameters on the small-signal behavior of a VSC-HVDC converter," *IEEE Trans. Power Del.*, vol. 29, no. 5, pp. 2287–2296, Oct. 2014.

[6] H. Liu et al., "Subsynchronous interaction between direct-drive PMSG based wind farms and weak ac networks," *IEEE Trans. Power Syst.*, vol. 32, no. 6, pp. 4708–4720, Nov. 2017.

[7] Du W, Dong W, Wang H. A Method of Reduced-Order Modal Computation for Planning Grid Connection of a Large-Scale Wind Farm[J]. *IEEE Trans. Sustain. Energy*, vol. 11, no. 3, pp. 1185-1198, July 2020.

[8] L. Harnefors, M. Bongiorno and S. Lundberg, "Input-Admittance Calculation and Shaping for Controlled Voltage-Source Converters," *IEEE Trans. Ind. Electron.*, vol. 54, no. 6, pp. 3323–3334, Dec. 2007.

[9] J. Sun, "Impedance-Based Stability Criterion for Grid-Connected Inverters," *IEEE Trans. Power Electron.*, vol. 26, no. 11, pp. 3075–3078, Nov. 2011.

[10] Kariniotakis G. N., Stavrakakis G, "Wind power forecasting using advanced neural networks models," *IEEE Trans. Energy Conversion*, vol. 11, no. 4, pp. 762-767, Dec. 1996.

[11] FAN Shu, LIAO J R, YOKOYAMA R, et al. Forecasting the wind generation using a two-stage network based on meteorological information. *IEEE Trans. Energy Conversion*, vol. 24, no. 2, pp. 474-482, June 2009.

[12] Dorfler F, Bullo F. Kron Reduction of Graphs with Applications to Electrical Networks[J]. *IEEE Transactions on Circuits & Systems I Regular Papers*, vol. 60, no. 1, pp. 150-163, Jan. 2013.

[13] D. Henrion and J.-B. Lasserre, "Convergent relaxations of polynomial matrix inequalities and static output feedback," *IEEE Trans. Autom. Control*, vol. 51, no. 2, pp. 192-202, Feb. 2006.

978-1-6654-0823-3/22/$31.00 ©2022 IEEE